Multi-Objective Optimum Design of Energy Systems based on Particle Swarm Optimization

M.J. MAHMOODABADI[1], A.R. GHAVIMI[2], AND F. JAMADI[3]

[1] *Department of Mechanical Engineering, Sirjan University of Technology, Sirjan, Iran.*
[2] *Faculty of Mechanical Engineering, University of Tabriz, Tabriz, Iran.*
[3] *Department of physics, Sirjan University of Technology, Sirjan, Iran.*
[*] *Corresponding author: mahmoodabadi@sirjantech.ac.ir*

Manuscript received January 08, 2018;Revised April 19, accepted June 08,2018. Paper no. JEMT-1801-1057

Improving and enhancing methodologies for efficient and effective design of energy systems is one of the most important challenges that energy engineers face. In this work, a multi-objective particle swarm optimization (PSO) algorithm is applied for a highly constrained cogeneration problem which named CGAM problem as a standard cycle to verify all optimization methods. The regarded objective functions are the exergetic efficiency that should be maximized and the total cost rate that should be minimized, simultaneously. In order to determine the polar effects of the pressure ratio and the turbine inlet temperature on the specified objective functions, a sensitivity analysis is performed. The related Pareto fronts with different values of equivalence ratios, unit costs of fuel, and NOx emissions represented and their effects on the system studied. Furthermore, the comparison between the obtained results andother evolutionary algorithms demonstrates the superiority and efficiency of the considered multi-objective particle swarm optimization algorithm.

keywords: *Multi-objective optimization; Highly constrained thermal system; Exergetic efficiency; Total cost rate; Particle swarm optimization; Pareto design.*

http://dx.doi.org/10.22109/jemt.2018.114074.1057

1. INTRODUCTION

Some specialists in the field of exergoeconomic [1,2] decided to develop optimization methods on the standard problem. This problem, which is an acronym of the aforementioned scientists' name, is known as the CGAM problem. In general, the CGAM problem is a standard cycle to verify all optimization methods. Objectives involved in the optimum design process are considered as: thermodynamical aspect (e.g. maximum efficiency, minimum fuel consumption, and minimum irreversibility), economical aspect (e.g. the minimum cost per unit of time and maximum profit per unit of production), and environmental aspect (e.g. limited emissions and minimum environmental impact) [3]. In order to decrease the computational cost and time, some researchers have defined the environmental objective in cost terms and added it to the thermodynamic objective function. Hence, a new objective function called thermoenvironomic objective function has been created [4]. This optimization problem could be solved using the evolutionary algorithms. For instance, Hammache et al. have implemented a multi-objective and self-adaptive algorithm to optimize the CGAM problem [5]. In [6], a particle swarm optimization algorithm has been utilized for optimization of this problem. The cost function of investment and fuel has been introduced as a single-objective function. So, CGAM problem has been optimized economically. In [7], a multi-objective optimization method based on artificial bee colony has been implemented on power and heating systems. In [8], a multi-objective optimization of solar-hybrid cogeneration cycle as CGAM problem has been performed. In [9], a new hybrid optimization algorithm has been proposed in act of multi-objective optimization for power and heating systems. In [10], thermoeconomic optimization of gas turbine cogeneration plants has been investigated. In [11], the Monte Carlo method has been utilized for economic optimization of cogeneration CGAM systems. In [12], the efficient symbolic search has been successfully applied for cost-optimal planning.

Particle swarm optimization has been originally introduced by Kennedy and Eberhart [13] and is reported as one of the most successful optimization algorithms [14–17]. In the recent

years, several approaches have been proposed to develop this algorithm through single-objective [18–20] and multi-objective optimization problems [21–24]. Spatially, in [25, 26], the multi-objective particle swarm optimization has been modified in two stages. At the first stage, particle swarm optimization has been combined with two novel convergence and divergence operators. At the second stage, two mechanisms have been used to produce the set of Pareto optimal solutions which have good convergences, diversities, and distributions. At the first mechanism, a new leader selection method which uses the periodic iteration and the concept of the number of particle's neighbors has been defined. At the second mechanism, an adaptive elimination method has been employed to limit the number of non-dominated solutions in the archive. In these references, several complex test functions and real-world problems have been used to challenge the proposed optimization algorithm. The results have illustrated that it performs very well in implementation of single-objective and multi-objective problems considering aspects of results accuracy, solutions diversity, and convergence speed. Hence, this successful algorithm is also implemented this paper to accomplish the Pareto fronts of a modified CGAM problem.

2. OPTIMIZATION ALGORITHM

The proper selection of design variables is one of the most important issues in the aspect of CGAM problems. Therefore, a novel multi-objective particle swarm optimization is applied in this paper to overcome mentioned problem. Previous researches illustrate that this optimization method can be successfully used to obtain the Pareto frontiers of non-commensurable objective functions for the design of linear state feedback controllers [25] and suspension systems of vehicle vibration models [26]. This method is a combination of particle swarm optimization, convergence, and divergence operators. Moreover, a periodic leader selection method and an adaptive elimination technique are implemented to prune the archive in this algorithm named periodic CDPSO. In the following, particle swarm optimization, convergence and divergence operators, periodic leader selection, and adaptive elimination techniques are described briefly.

A. Particle Swarm Optimization

Kennedy and Eberhart [13] proposed the population-based particle swarm optimization algorithm inspired from the simulation of the social behavior of birds within a flock. Mainly, in the problems with real number design variable, particle swarm optimization is a very popular global optimizer [27, 28].

In this approach, the position of each particle is enhanced by using its own and neighbors experience. Let $\vec{x_i}(t)$ denote the position of particle i, at iteration t. The position of $\vec{x_i}(t)$ would be changed by adding the velocity $\vec{v_i}(t)$ to current position, i.e:

$$\vec{x_i}(t+1) = \vec{x_i}(t) + \vec{v_i}(t+1) \quad \textbf{(1)}$$

The velocity vector reflects the socially exchanged information that is generally defined as follows:

$$\vec{v_i}(t+1) = W\vec{v_i}(t) + C_1 r_1(\vec{x}_{pbest_i} - \vec{x_i}(t)) + C_2 r_2(\vec{x}_{gbest} - \vec{x_i}(t)) \quad \textbf{(2)}$$

where, $r_1, r_2 \in [0,1]$ are random values. C_1 is the cognitive learning factor and represents the attraction of the particle toward its own success. C_2 is the social learning factor and represents the attraction of the particle toward the success of the swarm. W is the inertia weight that controls the impact of the previous history of velocities with the current velocity of the particle. $\vec{x}_{pbest}$ is the personal best position of the particle i. $\vec{x}_{gbest}$ is the position of the best particle of the entire swarm.

B. Convergence Operator

A novel convergence formula is originally introduced in [25, 26] that contains four different positions of particles. Let $\rho \in [0,1]$ be a random number. If $\rho < P_C$ (P_C is the convergence probability) then, one of the following equations could be implemented to generate the new particle position $\vec{x_i}(t+1)$ from the old particle position $\vec{x_i}(t)$.

$$\vec{x_i}(t+1) = \vec{x}_{gbest} + \sigma_1\left(\frac{\vec{x}_{gbest}}{\vec{x_i}(t)}\right)(2\vec{x_i}(t) - \vec{x_j}(t) - \vec{x_k}(t)) \text{if } f(\vec{x_i}(t)) < f(\vec{x_j}(t)) \angle \text{and} f(\vec{x}_k(t)) \quad \textbf{(3)}$$

$$\vec{x_i}(t+1) = \vec{x}_{gbest} + \sigma_2\left(\frac{\vec{x}_{gbest}}{\vec{x_i}(t)}\right)(2\vec{x_j}(t) - \vec{x_i}(t) - \vec{x_k}(t)) \text{if } f(\vec{x_j}(t)) < f(\vec{x_i}(t)) \text{and} f(\vec{x}_k(t)) \quad \textbf{(4)}$$

$$\vec{x_i}(t+1) = \vec{x}_{gbest} + \sigma_3\left(\frac{\vec{x}_{gbest}}{\vec{x_i}(t)}\right)(2\vec{x_k}(t) - \vec{x_j}(t) - \vec{x_i}(t)) \text{if } f(\vec{x_k}(t)) < f(\vec{x_i}(t)) \text{and} f(\vec{x}_j(t)) \quad \textbf{(5)}$$

where particles $\vec{x_j}(t)$ and $\vec{x_k}(t)$ are selected from swarm by uniform selection method. $f(\vec{x}_i(t))$ illustrated the objective function value of particle $\vec{x_i}(t)$. σ_1, σ_2, and σ_3 are random numbers selected from and $\vec{x}_{gbest}$ is the best particle position of the entire swarm. After calculation of Equations (3) to (5), the superior particle between $\vec{x_i}(t)$ and $\vec{x_i}(t+1)$ should be selected.

C. Divergence Operator

A novel divergent formulation originally proposed in [25,26] that is simply controlled mutation operator and provides a possible leap for a chosen particle $\vec{x_i}(t)$. Let $\vartheta \in [0,1]$ be a random number. If $\vartheta < P_D$, (P_D is the divergence probability) and particle $\vec{x_i}(t)$ has been not enhanced by the convergence operator, then the following equation is used to calculate a new particle.

$$\vec{x_i}(t+1) = Normrand\ (\vec{x_i}(t), S_D) \quad \textbf{(6)}$$

where $Normrand\ (\vec{x_i}(t), S_D)$ generates random numbers with the normal distribution from mean $\vec{x_i}(t)$ and standard deviation S_D.

D. Periodic Leader Selection

For solving single-objective optimization problems by PSO approach, $\vec{x}_{gbest}$ is implemented as a leader to update the position of the particles. However, in the case of multi-objective optimization problems, each particle might have a set of different leaders (non-dominate solutions) which only one of them can be selected. In [25,26], the authors described a leader selection technique based on density measures. This means that a neighborhood radius ($R_{neighborhood}$) is defined for leaders. Two leaders

are considered as each of their neighbors if the Euclidean distance (measured in the objective domain) between them be less than $R_{neighborhood}$. In act of using this definition, the number of neighbors in the set of all members is calculated and the particle with fewer neighbors is assigned as the leader. This prosess should be repeated in each period. In fact, the maximum iteration is divided into several equal periods and each period has the same generation T as follows.

$$\text{maxit} = \text{numberofperiods} \times \text{T} \tag{7}$$

Furthermore, before each iteration of a period it should be checked that if a particle dominates as a leader, this particle would be consider and update as the new leader. This algorithm which named periodic multi-objective optimization, allows performing initialization, inertia weight, and selection of learning factors in each period. Here, the following equations have been utilized for initialization, inertia weight, and cognitive social learning factors in each period [25,26].

$$x_i\left(0\right) = Normrand\left(\vec{x}_{gbest}, P_I\right) \tag{8}$$

$$v_i\left(0\right) = \overrightarrow{rand} \tag{9}$$

$$W = W_1 + \left(W_2 - W_1\right)\left(\frac{it}{T} - fix\left(\frac{it-1}{T}\right)\right) \tag{10}$$

$$c_1 = 0 \tag{11}$$

$$C_2 = C_{2i} + \left(C_{2f} - C_{2i}\right)\left(\frac{it}{T} - fix\left(\frac{it-1}{T}\right)\right) \tag{12}$$

where $x_i(0)$ and $v_i(0)$ are the initial position and initial velocity of particle i, $Normrand\left(\vec{x}_{gbest}, P_I\right)$ generates random numbers with the normal distribution, mean $\vec{x}_{gbest}, P_I$, and standard deviation P_I. $\overrightarrow{rand}$ is a vector of random values between 0 and 1. W_1 and W_2 denote the initial and final values of the inertia weight in each period, respectively. $C_{(2i)}$ and $C_{(2f)}$ are the initial and final values of the social learning factor in each period, respectively. Variable it represents the current iteration number and T is the number of iterations in a period. $fix(\frac{it-1}{it})$ is a function that rounds $fix(\frac{it-1}{it})$ to the nearest integer number toward zero.

E. Adaptive Elimination Technique

In the multi-objective optimization process, if all of the non-dominate solutions which obtained in every iteration are kept in the archive, then its size would increase rapidly. In order to prevent this issue, the size of the archive has been bounded through the proposed adaptive elimination technique in [25,26]. In the technique used to prune the archive, each particle in the archive has an elimination radius R_e. IF the Euclidean distance between two particles is less than R_e, then one of them will be removed.

$$R_e = \frac{it}{\zeta \times \max it} \tag{13}$$

where *zeta* is a positive constant.

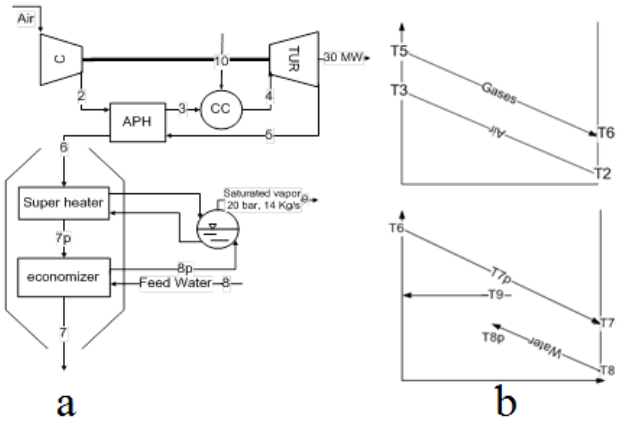

Fig. 1. A schematic of the CGAM problem

3. MODIFIED CGAM PROBLEM

A. Thermodynamic Model

The CGAM problem is related to a cogeneration plant with delivery of 30 MV of electricity and 14 (kg/s) of saturated steam at 20 bars illustrated in Fig. 1a. Moreover, the temperature variations of the air preheated and heat recovery steam generator are depicted in Fig. 1b. The conditions of the considered environment are regarded as $T_o = 298.15$ and $P_o = 1.013$ bar and the temperature of the exhaust gases are bounded as $T_7 > 400$K; and also, $T_1 = 298.15, p_1 = 1.013bar, T_8 = 298.15K, p_8 = 20$ bar, $T_10 = 298.15K, p_10 = 12bar, T_3 = 850K, T_4 = 1520K$, $\eta_get = 0.847$,and $\eta_c = 0.878$. Other conditions and specifications are as follows. All processes considered as steady-state, the air and combustion gases are ideal gas, the pressures drop of the combustion chamber, air preheater, and Heat Recovery Steam Generator (HRSG) are known, the heat loss of the combustion chamber is 2% of the Lower Heating Value (LHV), and the other presses are considered as adiabatic.

If the initial conditions of the cycle are considered as the same as [29], then the result of the thermodynamic modeling would be obtain according to Table 1.

Fig. 2 represents the values of the exergetic efficiency with changing turbine inlet temperature and pressure ratio. There is an optimum value of the pressure ratio for any specified turbine inlet temperature that maximizes the exergetic efficiency. As it can be seen, increasing turbine inlet temperature absolutely improves the amount of the exergetic efficiency.

Exergy destruction of various components has been demonstrated in Fig. 3. From this figure, the most exergy destruction belongs to the combustion chamber and its irreversibility is notable. There is a vast amount of heat transfer in Heat Recovery Steam Generator (HRSG) between gas mixture and steam and it has the greatest exergy destruction after the combustion chamber.

B. Economic Model

In this section, the rate of costs for the equipment has been determined. At first, items 1 to 5 in Table 2 represent the equations to calculate the purchased cost for the components. Where m_a, m_g,and m_{st} are the mass flow rates of air, gas, and steam, respectively. h_5 andh_6 are the specific enthalpies of streams 5 and 6. ΔT is the log mean temperature difference. $\dot{Q}_{SH}$ and $\dot{Q}_{EV}$ represent the rate of the heat transfer in the preheated economizer and the

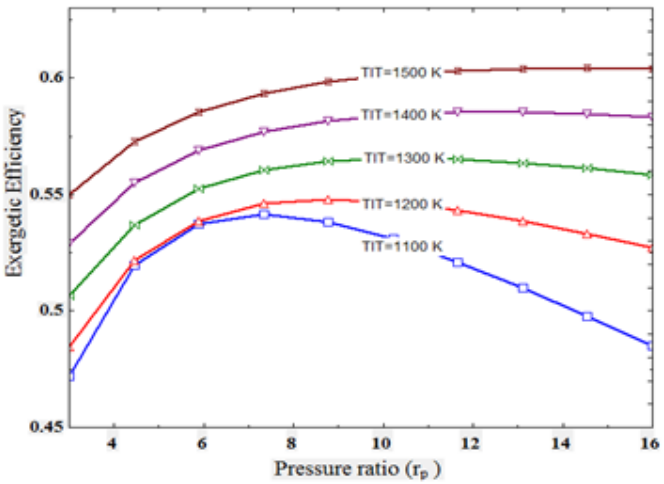

Fig. 2. The effects of the pressure ratio (r_p) and Turbine Inlet Temperature (TIT) on the exergetic efficiency.

Table 1. Thermodynamic properties of CGAM cycle for r_p =10 and TIT=1520 K.

State	$T_i(K)$	$\dot{m}_i(Kg/s)$	$P_i(KPa)$	$e_i(Kj/Kg)$
1	298.2	90.19	101.300	0
2	611.4	90.19	1.013×10^6	27337
3	850	90.19	9.620×10^6	41338
4	1520	91.83	925882	100699
5	1008	91.83	109900	38286
6	791.6	91.83	108.12	21640
7	423.8	91.83	101325	3073
8	298.2	14	2.000×10^6	26.67
9	482.5	14	2.000×10^6	12794
10	298.2	1.623	1.216×10^6	84464

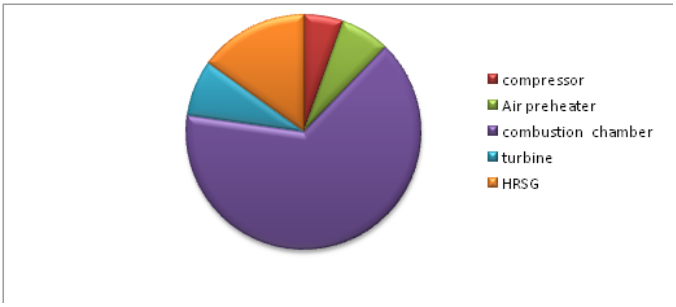

Fig. 3. The exergy destruction of the various components in the CGAM problem.

evaporator, respectively. The values of the constants are given in [29].

The investment cost flow rate $(\dot{Z}_l)$ is given in the item 6 of the Table 2. Where Z_i is the purchased cost of the *ith* component ($), CRF is the annual capital recovery factor (CRF=18.2 %), N represents the number of the hours of plant operation per year ($N = 8000h$), and ϕ is the maintenance factor ($\phi = 1.06$).

The fuel cost flow rate $(\dot{C}_F)$ is given by the item 7 of the Table 2. For the optimization process of the CGAM problem, the objective function is total cost flow rate $(\dot{C}_T)$ as the sum of the investment cost flow rate $(\dot{Z}_T)$ and fuel cost flow rate $(\dot{C}_F)$ (item 8 of the Table 2).

Table 2. The formulation of the economic modeling of the considered CGAM problem [29].

Item	Parameter	Formulation
1	Compressor	$Z_{AC} = \left(C_{11}\frac{\dot{m}_{air}}{C_{12}-\eta_{AC}}\right) r_{cp} log\,(r_{cp})$
2	Combustion Chamber	$Z_{CC} = \left(C_{21}\frac{\dot{m}_{air}}{C_{22}-p_4/p_3}\right)[1+\exp\,(C_{23}T_4 - C_{24})$
3	Turbine	$Z_{AC} = \left(C_{31}\frac{\dot{m}_{air}}{C_{32}-\eta_{st}}\right)\log\left(\frac{p_4}{p_5}\right)[1+\exp\,(C_{33}T_4 - C_{34})$
4	Air preheater	$Z_{AP} = \left(C_{41}\frac{\dot{m}_s(h_5-h_6)}{UAT}\right)$
5	Heat-recovery steam generator	$Z_{ap} = C_{51}\left(\left(\frac{\dot{Q}_{ph}}{\Delta T_{LPH}}\right)^{0.8} + \left(\frac{\dot{Q}_{ph}}{\Delta T_{LEV}}\right)^{0.8}\right) + C_{52}\dot{m}_{st} + C_{53}\dot{m}_s^{1.2}$
6	Investment cost flow rate	$\dot{Z}_l = Z_i \times CRF \times \varphi \times (N \times 3600)$
7	Fuel cost flow rate	$\dot{C}_F = \dot{m}_f \times c_f \times LHV$
8	Total cost flow rate	$\dot{C}_T = \dot{C}_f + \sum_k \dot{Z}_k$

C. Environmental Model

The adiabatic flame temperature in the primary zone of the combustion chamber is represented in item 1 of Table 3. Where π denotes a dimensionless pressure p/p_{ref} (p is the combustion pressure p_3 and $p_{ref} = 1.013$ bar). θ is a dimensionless temperature T/T_{ref} (T is the inlet temperature T_3 and T_{ref}=300 K). Ψ is the atomic ratio ($\Psi = 4$, the fuel is considered as pure methane). In order to have an accurate prediction, four sets of constants in the following ranges are considered.

$$0.3 \leq \phi \leq 1.0, \quad 0.92 \leq \theta \leq 2.0 \tag{14}$$

$$0.3 \leq \phi \leq 1.0, \quad 2 \leq \theta \leq 2.0 \tag{15}$$

$$1 \leq \phi \leq 1.6, \quad 0.92 \leq \theta \leq 2.0 \tag{16}$$

$$0.3 \leq \phi \leq 1.6, \quad 0.92 \leq \theta \leq 3.2 \tag{17}$$

This adiabatic flame temperature is used for the semi-analytical correlations to determine the pollutant emissions as indicated in item 2 to 4 in Table 3 [31]. where is the residence time in the combustion zone (for s=0.002 s), T_pz is the primary zone combustion temperature, p_3 is the combustor inlet pressure, and $\Delta p_3/p_3$ is the non-dimensional pressure drop in the combustor ($\Delta p_3/p_3 = 0.05$). Note that the primary zone temperature is used in the NO_x correlation instead of the stoichiometric temperature. Since, the maximum attainable temperature in premixed flames is T_{pz} [32]. C_{CO2} and C_{NOx} are regarded equal to 0.02086 $/kg CO and 6.853 $/kg $/NO$_x$, respectively.

The effect of the pressure ratio and Turbine Inlet Temperature (TIT) on the total cost rate ($/s) is represented in Fig. 4. There is an optimum r_p for any specified TIT that minimizes total cost rate. As can be seen, increasing TIT absolutely degrades the value of the total cost rate.

4. MULTI-OBJECTIVE OPTIMIZATION OF THE CGAM PROBLEM

A. Objective Functions and Design Variables

Three objective functions for this problem are considered as: 1) the total exergetic efficiency must be maximized, 2) the total cost

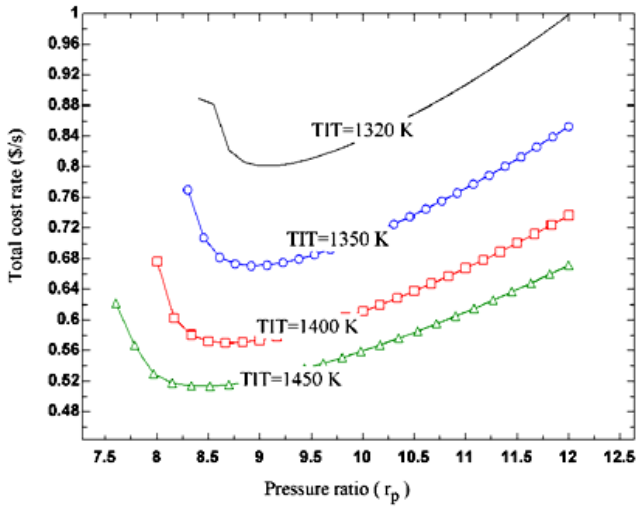

Fig. 4. The effects of the pressure ratio (r_p) and Turbine Inlet Temperature (TIT) on the total cost rate.

Table 3. The formulation of the environment modeling of the considered CGAM problem [30].

Item	Formulation
1	$T_{pz} = A\sigma^a \times \exp(\beta(\sigma+\lambda)^2)\pi^x\theta^y\Psi^z$
2	$NO_x = \left(\frac{0.15E16\times\tau^{0.5}\times\exp(-\frac{71100}{T_{pz}})}{p_3^{0.05}(\Delta P_3/P_3)^{0.5}}\right)$
3	$CO_2 = \left(\frac{0.179E9\times\exp(\frac{7800}{T_{pz}})}{p_3^2\times\tau\times(\Delta p_3/p_3)^{0.5}}\right)$
4	$Z_{AP} = \left(C_{41}\frac{m_g(h_5-h_6)}{U\Delta T}\right)$
5	$\dot{C}_{env} = c_{CO_2}\dot{m}_{CO_2} + c_{NO_x}\dot{m}_{NO_x}$

rate of the products (including investment and fuel cost rate) should be minimized, and 3) the specific rate of the pollutant emissions (environmental impact) should be minimized as represented in Table 4. Furthermore, the cost of pollution damage is directly added to the investment and fuel cost function.

Furthermore, for keeping the consistency with the original CGAM problem [1–4], the design variables have been selected as the compressor pressure ratio, efficiency of the air preheater, and temperature of the combustion products entering the gas turbine. These variables and their search ranges have been denoted in Table 4.

B. Results and Discussion

In this section, the multi-objective optimization of the CGAM problem would be perform by the periodic CDPSO and modify NSGA-II [33]. The specifications of these algorithms have been illustrated in Table 5.

The Pareto optimum fronts obtained via the periodic multi-objective CDPSO and NSGA-II for several fuel-to-air equivalence ratios are shown in Fig. 5. With increasing the equivalence ratio, the Pareto fronts shifted higher. It means that the effect of increasing the equivalence ratio is not desirable because the

Table 4. The formulation of the environment modeling of the considered CGAM problem [30].

Objective functions	$\varepsilon = (\dot{W}_{net} + \dot{m}_{st}(e_9 - e_8)/\dot{m}_f\dot{e}_{fuel}$	Exergetic objective function
	$\dot{C}_{total} = \dot{C}_f + \sum_k \dot{Z}_k + \dot{C}_{env}$	Thermoenvironomic objective function
Design variables	$7 < \frac{P_2}{P_1} < 16$	The compressor pressure ratio
	$0.6 < \varepsilon < 0.9$	The efficiency of the air preheater
	$1400 < T_4 < 1650$	The temperature of the combustion products entering the gas turbine

Table 5. The specifications of the algorithms applied to the multi-objective optimization process.

Algorithm	Population size	Maximum iteration (generation)	Setting parameters
Modified NSGA-II [33]	30	90	Crossover probability = 0.9; Mutation probability = 0.01; Crowding distance faction = 0.01
Periodic CDPSO	30	90	$w_1 = 0.9; w_2 = 0.4; C_1 = 0; T = 7;$ $\zeta = 300; C_{2i} = 0.5; C_{2f} = 2.5;$ $P_c = 0.45; P_D = 0.05; S_D = 0.4;$ $P_I = 0.04; R_{neighborhood} = 0.04$

cost rate will increase. Moreover, the superiority of the periodic CDPSO method can be clearly observed in this figure, especially for the greater values of the equivalence ratios.

Fig. 6 depicts obtained Pareto fronts using the NSGA-II and periodic CDPSO in $\phi = 0.64$ for the effect of different unit costs of fuel. By increasing the unit costs of fuel, the Pareto fronts shifted higher. It means that the increasing the unit costs of fuel is not desirable because it causes the increasing of the cost rate. In this figure, uniformity of the obtained Pareto front by the periodic CDPSO in comparison with the NSGA-II is highly significant.

Fig. 7 shows the effect of different values of NO_x emission on the Pareto diagram for $\phi = 0.64$. As it can be seen from this figure, the periodic CDPSO chart can provid more optimum solutions in comparison with NSGA-II. Further, increasing the value of NO_x emission leads to shifting the Pareto fronts up.

Fig. 8 illustrates the effect of pressure ratio on the objective functions in $\phi = 0.64$. As it can be seen from this figure, the optimum pressure ratios are in the range of 8.2 to 9 where there are maximum efficiency and minimum total cost rate.

Fig. 9 represents the Pareto fronts for the effect of turbine inlet temperature (K) on the objective functions in $\phi = 0.64$. This figure illustrates that the optimum turbine inlet temperatures are located in the range of 1600 K to 1640 K where there are maximum efficiency and minimum total cost rate.

5. CONCLUSION

Aim to overcome complexity and dimensionality of real-world problems, it needed to improve the efficiency and accuracy of the multi-objective particle swarm optimization algorithm. Therefore, the successful periodic CDPSO algorithm has been applied to optimize the modified CGAM problem involving two-objective functions. The simulation results and solution depicted that the reduction value of the equivalence ratio improves the system economic performance via rising the cost rate. Moreover, increasing the NO_x emission and the unit costs of fuel lead to shifting the optimum Pareto fronts up and rising the case rate. Further, the results demonstrat the robustness of the periodic CDPSO to compute the Pareto optimum fronts with excellent convergence and distribution in all cases. Furthermore, the results prove that the periodic multi-objective optimization

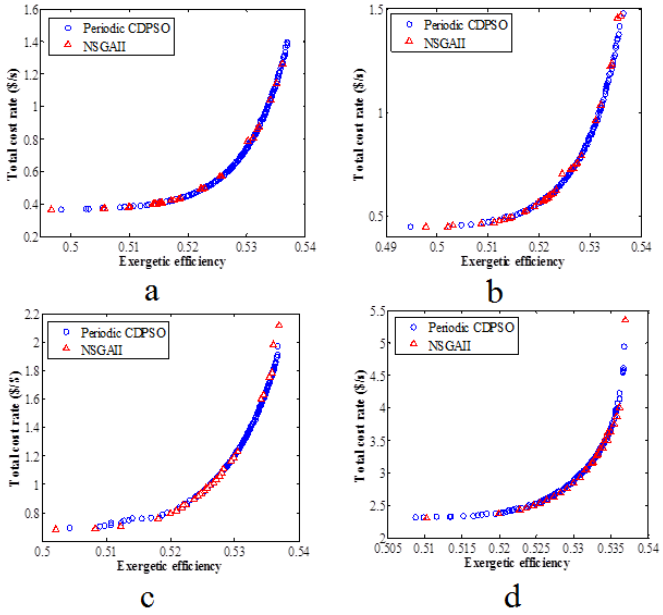

Fig. 5. The Pareto fronts obtained by the NSGA-II and periodic multi-objective CDPSO for the different equivalence ratios (a)$\phi = 0.5$, (b) $\phi = 0.6$, (c) $\phi = 0.64$, and (d) $\phi = 0.7$.

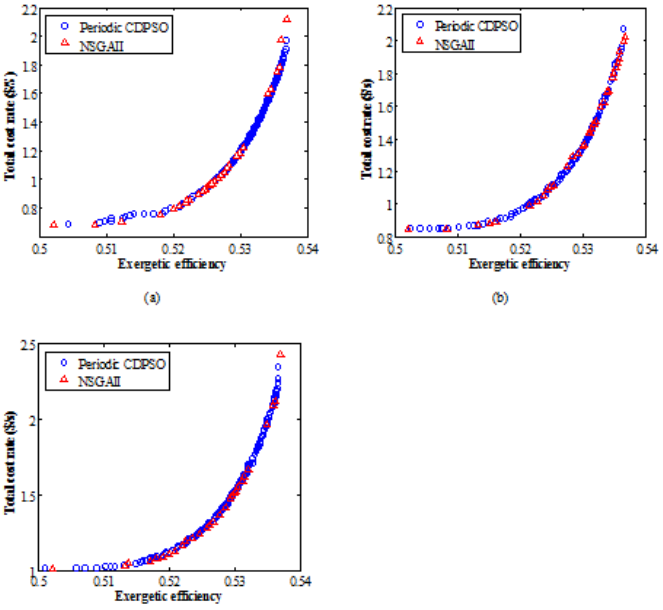

Fig. 6. The Pareto fronts obtained by the NSGA-II and periodic multi-objective CDPSO for the different unit costs of fuel in $\phi = 0.64$, (a) $C_f = 0.004$, (b) $C_f = 0.006$, and (c) $C_f = 0.008$.

algorithm can find better solutions compared to the NSGA-II.

REFERENCES

1. C. A. Frangopoulos, "Application of the thermoeconomic functional approach to the CGAM problem", Energy, vol. 19, no. 3, pp. 323-342, 1994.

2. G. Tsatsaronis, and J. Pisa, "Exergoeconomic evaluation and optimization of energy systems- appliocation to the CGAM problem", Energy, vol. 19, no. 3, pp. 287-321, 1994.

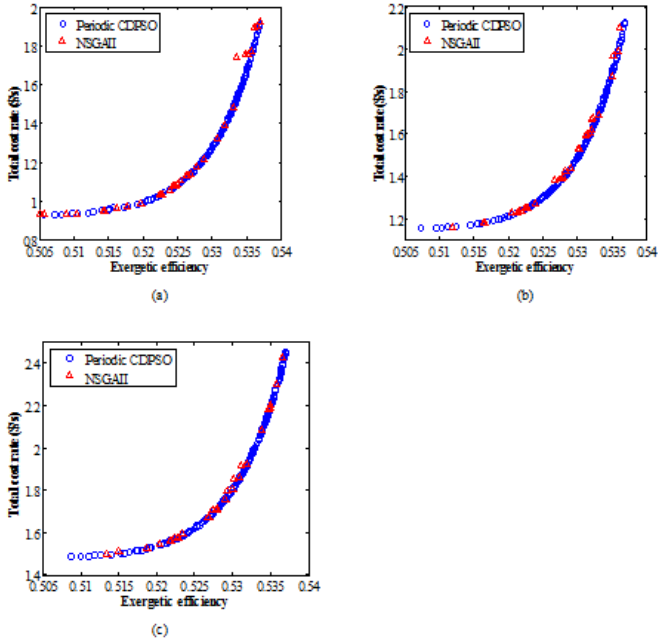

Fig. 7. The Pareto fronts obtained by the NSGA-II and periodic multi-objective CDPSO for the different NOx emission in $\phi = 0.64$, (a) NO_x emission=0.05(gr/s), (b)NO_x emission=0.07(gr/s), and (c) NO_x emission=0.1(gr/s).

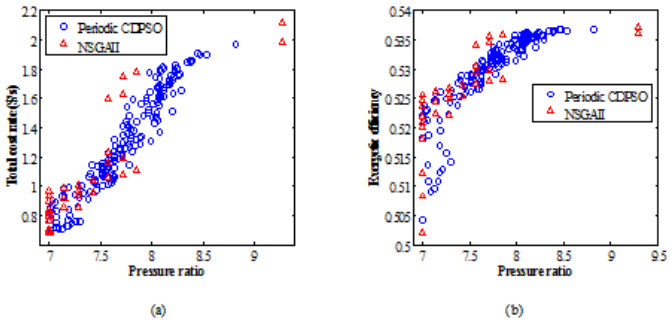

Fig. 8. The values of pressure ratio for Pareto optimum points in $\phi = 0.64$ for (a) total cost rate, (b) exergetic efficiency.

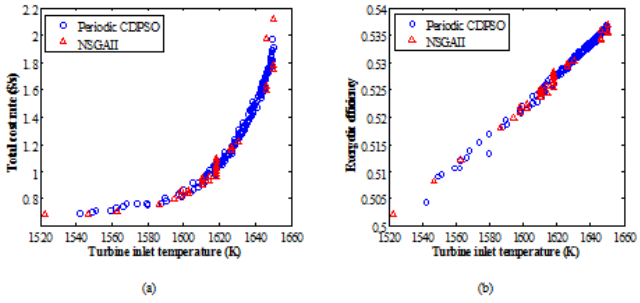

Fig. 9. The values of turbine inlet temperature for Pareto optimum points in $\phi = 0.64$ for (a) total cost rate, (b) exergetic efficiency.

3. A. Toffolo, and A. Lazzaretto, "Evolutionary algorithms for multi-objective energetic and economic optimization of thermal system design", Energy, vol. 27, no. 6, pp. 549–67, 2002.

4. A. Lazzaretto, and A. Toffolo, "Energy, economy and environment as objectives in multi-criterion optimization of thermal systems design", Energy, vol. 29, no. 8, pp. 1139–1157, 2004.

5. G. G. Dimopoulos, and C. A. Frangopoulos, "Optimization of energy systems based on evolutionary and social metaphors", Energy, vol. 33, no. 2, pp. 171–179, 2008.

6. A. Hammache, M. Benali, and F. Aubé, "Multi-objective self-adaptive algorithm for highly constrained problems: Novel method and applications", Applied Energy, vol. 87, pp. 2467–2478, 2010.

7. K. Atashkari, N. NarimanZadeh, A.R. Ghavimi, M.J. Mahmoodabadi, and F. Aghaienezhad, "Multi-objective optimization of power and heating system based on artificial bee colony", IEEE International Symposium on Innovations in Intelligent Systems and Applications, Istanbul, Turkey, pp. 64–68, 2011.

8. R. Soltania, P. Mohammadzadeh Keleshtery, M. Vahdati, M.H. KhoshgoftarManesh, M.A. Rosen, and M. Amidpour, "Multi-objective optimization of a solar-hybrid cogeneration cycle: Application to CGAM problem", Energy Conversion and Management, vol. 81, pp. 60-71, 2014.

9. M.J. Mahmoodabadi, A.R. Ghavimi, and S.M.S. Mahmoudi, "Optimization of power and heating systems based on a new hybrid algorithm", Alexandria Engineering Journal, vol. 54, pp. 343-350, 2015.

10. R. Karaali, and İ.T. Öztürk, "Thermoeconomic optimization of gas turbine cogeneration plants", Energy, vol. 80, pp. 474-485, 2015.

11. M. Momen, M. Shirinbakhsh, A. Baniassadi, and A. Behbahani-nia, "Application of Monte Carlo method in economic optimization of cogeneration systems-Case study of the CGAM system", Applied Thermal Engineering, vol. 104, pp. 34-41, 2016.

12. Á. Torralba, V. Alcázar, P. Kissmann, and S. Edelkamp, "Efficient symbolic search for cost-optimal planning", Artificial Intelligence, vol. 242, pp. 52-79, 2017.

13. J. Kennedy, and R.C. Eberhart, "Particle swarm optimization", Proceedings of the IEEE International Conference on Neural Networks IV, Piscataway, Australia, pp. 1942–1948, 1995.

14. Z. Zhan, J. Zhang, Y. Li, and H.S. Chung, "Adaptive particle swarm optimization", IEEE Transactions on Systems, Man and Cybernetics, Part-B, vol. 39, no. 6, pp. 1362–1381, 2009.

15. Y. Shi, H. Liu, L. Gao, and G. Zhang, "Cellular particle swarm optimization", Information Sciences, vol. 181, no. 20, pp. 4460–4493, 2011.

16. M. Bisheban, M.J. Mahmoodabadi, and A. Bagheri, "Partitioned particle swarm optimization", Applied and Computational Mathematics, vol. 2, no. 3, pp. 1-10, 2013.

17. M.J. Mahmoodabadi, Z. Salahshoor Mottaghi, and A. Bagheri, "HEPSO: High exploration particle swarm optimization", Information Sciences, vol. 273, pp. 101–111, 2014.

18. Z. Chen, R. Xiong, and J. Cao, "Particle swarm optimization-based optimal power management of plug-in hybrid electric vehicles considering uncertain driving conditions", Energy, vol. 96, pp. 197-208, 2016.

19. P. Shen, Z. Zhao, X. Zhan, and J. Li, "Particle swarm optimization of driving torque demand decision based on fuel economy for plug-in hybrid electric vehicle", Energy, vol. 123, pp. 89-107, 2017.

20. A. Lorestani, and M.M. Ardehali, "Optimal integration of renewable energy sources for autonomous tri-generation combined cooling, heating and power system based on evolutionary particle swarm optimization algorithm", Energy, vol. 145, pp. 839-855, 2018.

21. G. Gary. Yen, and Wen Fung Leong, "Dynamic multiple swarms in multi-objective particle swarm optimization", IEEE Transactions on Systems, Man, and Cybernetics, part-A, Systems and Humans, vol. 39, no. 4, pp. 890–911, 2009.

22. C.K. Goh, K.C. Tan, D.S. Liu, and S.C. Chiam, "A competitive and cooperative co-evolutionary approach to multi-objective particle swarm optimization algorithm design", European Journal of Operational Research, vol. 202, no. 1, pp. 42–54, 2010.

23. S.N. Omkar, A. Venkatesh, and M. Mudigere, "MPI-based parallel synchronous vector evaluated particle swarm optimization for multi-objective design optimization of composite structures", Engineering Applications of Artificial Intelligence, vol. 25, no. 8, pp. 1611–1627, 2012.

24. M.J. Mahmoodabadi, M. Taherkhorsandi, and A. Bagheri, "Optimal robust sliding mode tracking control of a biped robot based on ingenious multi-objective PSO", Neurocomputing, vol. 124, pp. 194–209, 2014.

25. M.J. Mahmoodabadi, A. Bagheri, S. Arabani-Mostaghim, and M. Bisheban, "Simulation of stability using Java application for Pareto design of controllers based on a new multi-objective particle swarm optimization", Mathematical and Computer Modelling, vol. 54, no. 5-6, pp. 1584–1607, 2011.

26. M.J. Mahmoodabadi, A. Bagheri, N. Nariman-zadeh, and A. Jamali, "A new optimization algorithm based on a combination of particle swarm optimization, convergence and divergence operators for single-objective and multi-objective problems", Engineering Optimization, vol. 44, no.10, pp. 1167–1186, 2012.

27. A.P. Engelbrecht, "Fundamentals of computational swarm intelligence", John Wiley Sons, 2005.

28. A. Farokhi, and M.J. Mahmoodabadi, "Optimal fuzzy inverse dynamics control of a parallelogram mechanism based on a new multi-objective PSO", Cogent Engineering, vol. 5, no. 1, pp. 1-20, 2018.

29. A. Bejan, G. Tsatsaronis, and M. Moran, "Thermal design and optimization", New York, John Wiley, 1996.

30. Ö.L. Gülder, "Flame temperature estimation of conventional and future jet fuels", Journal of Engineering for Gas Turbines and Power, vol. 108, no. 2, pp. 376–380, 1986.

31. N.K. Rizk, and H.C. Mongia, "Semianalytical correlations for NOx, CO and UHC emissions", Journal of Engineering for Gas Turbines and Power, vol. 115, no. 3, pp. 612–619, 1993.

32. A.H. Lefebvre, "Gas turbine combustion Ann. Arbor (MI)", Edwards Brothers, 1998.

33. K. Atashkari, N. Nariman-Zadeh, M. Golcu, A. Khalkhali, and A. Jamali, "Modelling and multi-objective optimization of a variable valve-timing spark-ignition engine using polynomial neural networks and evolutionary algorithms", Energy Conversion and Management, vol. 48, no. 3, pp. 1029–1041, 2007.